Propagation of Nonlinear Flood Waves in Rivers

Sergio E. Serrano[1]

Abstract: The propagation of flood waves in rivers is governed by the Saint Venant equations. Under certain simplifying assumptions, these nonlinear equations have been solved numerically via computationally intensive, specialized software. There is a cogent need for simple analytical solutions for preliminary analyses. In this paper, new approximate analytical solutions to the nonlinear kinematic wave equation and the nonlinear dynamic wave equations in rivers are presented. The solutions have been derived by combining Adomian's decomposition method (ADM), the method of characteristics, the concept of double decomposition, and successive approximation. The new solutions compare favorably with independent simulations using the modified finite-element method and field data at the Schuylkill River near Philadelphia. The time to peak calculated by the analytical and numerical methods is in excellent agreement. There appears to be some minor differences in the peak magnitude and recession limb, possibly because of numerical dissipation. Including the momentum equation in the analysis causes a decrease in the magnitude of the flow rate at all times. Except for the flood peak, the nonlinear analytical solution exhibits lower flow rates than the numerical solution. The numerical solution also shows higher dispersion. The new analytical solutions are easy to apply, permit an efficient preliminary forecast under scarce data, and an analytic description of flow rates continuously over the spatial and temporal domains. They may also serve as a potential source of reference data for testing new numerical methods and algorithms proposed for the open channel flow equations. The ADM nonlinear kinematic and nonlinear dynamic wave solutions exhibit the usual features of nonlinear hydrographs, namely, their asymmetry with respect to the center of mass, with sharp rising limbs and flatter recession limbs. Linear approximations of the governing equations usually miss these important features of nonlinear waves. The greatest portion of the magnitude of discharge is given by the initial nonlinear kinematic wave component, which implies that in the lower Schuylkill River the translational components dominate the propagation of flood waves, in agreement with previous research. The nonlinear dynamic wave better predicts the flow rate during peak times and especially during recession and low-flow periods. Thus, while both the nonlinear kinematic and the nonlinear dynamic wave models are based on simple approximate analytical solutions that are easy to implement, the nonlinear kinematic wave equation model requires less data and less computational effort. **DOI: 10.1061/(ASCE)HE.1943-5584.0001268.**

Author keywords: Nonlinear kinematic and dynamic flood waves; Analytical solutions; Mathematical models; Adomian's decomposition method.

Introduction

The propagation of flood waves in rivers is governed by the nonlinear Saint Venant equations. Under certain simplified assumptions, many models have been developed over the last several decades (e.g., de Almeida and Bates 2013; de Almeida et al. 2012; Philipp et al. 2012; Bates et al. 2010; Moramarco et al. 2008; Tsai and Yen 2004; Tsai 2003; Aronica et al. 1998; Cappelaere 1997; Lamberti and Pilati 1996; Singh and Aravamuthan 1996; Xia 1995; Dooge and Napiorkowski 1987; Hromadka and Yen 1986; Ponce 1986; Ferrick 1985; Ferrick et al. 1984; Vieira 1983; Morris and Woolhiser 1980; Ponce et al. 1978; Ponce and Simons 1977; Di Silvio 1969; Woolhiser and Liggett 1967; Lighthill and Whitham 1955). Most approaches to solving the resulting nonlinear equations use numerical methods or analytical solutions of the linearized equations. Numerical solutions (e.g., finite differences, finite elements) reduce the differential equations to a simpler system of algebraic equations, can handle irregular domain shapes, and may handle numerical approximations of the model nonlinearities (e.g., Kazezyilmaz-Alhan and Medina 2007; Jin and Fread 1997). However, numerical solutions yield the state variables at discrete nodes only (i.e., they require a grid), are computationally expensive, are difficult to program (i.e., they require specialized computer software), and often have difficulties with numerical instabilities and roundoff errors. There is a cogent need for simple analytical solutions of the nonlinear kinematic wave and the nonlinear dynamic wave equations in rivers for preliminary analyses under scarce data. Classical analytical solutions (e.g., Fourier series, Laplace transform) are simple to program, are usually stable, and offer a spatially and temporally continuous description of hydrologic variables. However, classical analytical solutions cannot handle nonlinearities. In this paper, the author introduces new solutions to the nonlinear kinematic wave and the nonlinear dynamic wave equations using an alternative method, namely, Adomian's decomposition method (ADM) (Adomian 1983, 1986, 1991, 1994, 1995), which offers the simplicity, stability, and spatial and temporal continuity of analytical solutions, in addition to the ability to handle system nonlinearities of numerical solutions. For a detailed introduction to the ADM, practical examples in hydrology, and computer programs, see Serrano (2010, 2011). Many studies have reported new solutions to a wide class of equations (ordinary, partial, differential, integral, integrodifferential, linear, nonlinear, deterministic, or stochastic) in a variety of fields such as mathematical physics, science, and engineering (e.g., Rach et al. 2013; Duan and Rach 2011; Rach 2008, 2012; Wazwaz 2000; Adomian 1991, 1994). For nonlinear

[1]Senior Scientist, HydroScience Inc., 1217 Charter Ln., Ambler, PA 19002. E-mail: hydroscience@earthlink.net

Note. This manuscript was submitted on March 10, 2015; approved on May 19, 2015; published online on July 6, 2015. Discussion period open until December 6, 2015; separate discussions must be submitted for individual papers. This paper is part of the ***Journal of Hydrologic Engineering***, © ASCE, ISSN 1084-0699/04015053(7)/$25.00.

equations in particular, decomposition is one of the few systematic solution procedures available (Adomian 1994).

In this paper, a new approximate analytical solution to the nonlinear dynamic wave equation is presented. Serrano (2006) used a one-term ADM expansion to derive an approximate analytical solution to the nonlinear kinematic wave equation. In this paper, the author introduces several mathematical modifications to derive a new approximate analytical solution to the nonlinear kinematic wave equation. Instead of a one-term decomposition, the method of double decomposition is used, and several terms, not just one. In addition, the new solution to the nonlinear kinematic wave equation is used as a first term in the solution to the nonlinear dynamic wave decomposition expansion. The new analytical solutions to the nonlinear kinematic wave and the nonlinear dynamic wave are verified with a numerical solution (the modified finite-element method), independently documented and published by Szymkiewicz (2010). The new solutions are also verified with field data at the Schuylkill River near Philadelphia.

Nonlinear Dynamic Wave Model

Under certain simplifying assumptions of the flow process in rivers, the Saint Venant equations have been solved via traditional numerical methods. The most important assumptions are the following: The flow is one dimensional. Water depth and velocity vary only in the longitudinal direction. This implies that the velocity is constant and the water surface is horizontal across any section perpendicular to the longitudinal axis. Flow is assumed to vary gradually along the river channel. Vertical momentum and vertical accelerations are neglected so that hydrostatic pressure prevails. The longitudinal axis of the river channel is approximated as a straight line. The bottom slope of the channel is small and the channel bed is fixed; the effects of scour and deposition are negligible. Resistance coefficients for steady uniform turbulent flow are applicable. The fluid is incompressible and of constant density throughout the flow. Under these assumptions, detailed derivations of the conservation and nonconservation form of the Saint Venant equations may be consulted in standard treatises. See, for example, Szymkiewicz (2010), Martin and McCutcheon (1999), Chow et al. (1988), and Singh (1996) for excellent descriptions and bibliographic summaries of solution approaches. The conservation form of the continuity equation is given by

$$\frac{\partial Q}{\partial x}+\frac{\partial A}{\partial t}=Q_L \tag{1}$$

where $Q(x,t)$ = flow rate (m^3/s); Q_L = lateral flow into the channel per unit length (m^2/s); x = distance (m) from a streamflow station with a known hydrograph; t = time (h); and A = flow cross-sectional area (m^2). Neglecting the wind shear, eddy losses, and the momentum of lateral flow, the conservation form of the momentum equation is given by (Chow et al. 1988)

$$\frac{1}{A}\frac{\partial Q}{\partial t}+\frac{1}{A}\frac{\partial}{\partial x}\left(\frac{Q^2}{A}\right)+g\frac{\partial y}{\partial x}-g(S_0-S_f)=0 \tag{2}$$

where y = water depth (m); $g=9.807$ is the gravitational acceleration (m/s^2); S_0 = channel bottom slope; and S_f = slope of the energy line. Consider initially a rectangular channel. Assuming Manning's formula is valid, the following expressions are useful (Chow 1959):

$$y=\frac{A}{B},\qquad S_f=\frac{n^2Q^2}{R^{4/3}A^2}=\frac{n^2(B+\frac{2A}{B})^{4/3}Q^2}{A^{10/3}} \tag{3}$$

where B = channel width at the water surface (m); n = Manning's roughness coefficient; and R = hydraulic radius (m). Neglecting hysteresis, the channel cross-sectional area is often expressed as

$$A=\propto Q^{\beta} \tag{4}$$

where α is a constant with dimensions ($m^{2-3\beta}s^{\beta}$); and β is a dimensionless constant. Combining Eqs. (1) and (2), and substituting Eqs. (3) and (4) into the resulting equation yields a dynamic wave equation given by

$$\begin{aligned}&L_xQ=Q_L-\propto\beta Q^{\beta-1}L_tQ+S_0-\frac{n^2}{\alpha^{10/3}}\left(B+2\propto\frac{Q^{\beta}}{B}\right)^{4/3}\\&Q^{2-(10\beta/3)}-\frac{\propto}{B}L_xQ^{\beta}-\frac{2-\beta}{2g\alpha^2(1-\beta)}L_xQ^{2-2\beta}-\frac{1}{g\propto Q^{\beta}}L_tQ,\\&Q(0,t)=Q_I(t),\qquad Q(x,0)=Q_I(0)\end{aligned} \tag{5}$$

where the operators $L_x=\partial/\partial x$, $L_t=\partial/\partial t$; and $Q_I(t)$ = inflow hydrograph at $x=0$.

An x-partial decomposition expansion may be obtained by operating with $L_x^{-1}=\int(\,)dx$ on both sides of Eq. (5)

$$\begin{aligned}Q=Q_Lx-L_x^{-1}F(Q)L_tQ+L_x^{-1}G(Q)+H(Q)+K(Q)\\+L_x^{-1}J(Q)L_tQ\end{aligned} \tag{6}$$

where the nonlinear functions

$$\begin{aligned}&F(Q)=\propto\beta Q^{\beta-1}\\&G(Q)=S_0-\frac{n^2}{\propto^{10/3}}(B+2\propto Q^{\beta}/B)^{4/3}Q^{2-10\beta/3}\\&H(Q)=-\frac{\propto}{\beta}Q^{\beta}\qquad K(Q)=-\frac{(2-\beta)}{2g\alpha^2(1-\beta)}Q^{2-2\beta}\\&J(Q)=-\frac{1}{g\propto Q^{\beta}}\end{aligned} \tag{7}$$

Now define the decomposition series $Q=\sum_{i=0}^{\infty}Q_i$ and the Adomian polynomials for the nonlinear functions in Eq. (7) as $F(Q)=\sum_{j=0}^{\infty}F_j$, $G(Q)=\sum_{j=0}^{\infty}G_j$, $H(Q)=\sum_{j=0}^{\infty}H_j$, $K(Q)=\sum_{j=0}^{\infty}K_j$, and $J(Q)=\sum_{j=0}^{\infty}J_j$. The Adomian polynomials may be calculated in a variety of ways (Rach et al. 2013; Duan and Rach 2011; Rach 2008; Wazwaz 2000; Adomian 1994). Hence, Eq. (6) becomes

$$\begin{aligned}Q=Q_Lx-L_x^{-1}\sum_{j=0}^{\infty}F_jL_t\sum_{i=0}^{\infty}Q_i+L_x^{-1}\sum_{j=0}^{\infty}G_j+\sum_{j=0}^{\infty}H_j\\+\sum_{j=0}^{\infty}K_j+L_x^{-1}\sum_{j=0}^{\infty}J_jL_t\sum_{i=0}^{\infty}Q_i\end{aligned} \tag{8}$$

Defining the first term in the series, Q_k, as composed of the first two terms in the right side of Eq. (8)

$$Q_k=Q_Lx-L_x^{-1}\sum_{j=0}^{\infty}F_jL_t\sum_{k=0}^{\infty}Q_k \tag{9}$$

Clearly, Q_k satisfies the kinematic wave equation given by

$$\begin{aligned}&\frac{\partial Q_k}{\partial x}+\propto\beta Q_k^{\beta-1}\left(\frac{\partial Q_k}{\partial t}\right)=Q_L,\\&Q_k(0,t)=Q_I(t),\qquad Q_k(x,0)=Q_I(0)\end{aligned} \tag{10}$$

To solve Eq. (10), let us extend the approach of Serrano (2006). The characteristics equation of Eq. (10) is determined by (Jeffrey 2003)

$$\frac{dt}{dx} = \propto \beta Q_k^{\beta-1} \tag{11}$$

and the compatibility condition is

$$\frac{dQ_k}{dx} = Q_L \tag{12}$$

Integrating Eq. (12) along a characteristic that passes through the point $(0, \xi)$ yields

$$Q_k(x,t) = Q_I(\xi) + Q_L x \tag{13}$$

Integrating the characteristic Eq. (11) gives

$$t = \alpha\beta Q_k^{\beta-1}(\xi)x + \xi \tag{14}$$

Using Eq. (13) to eliminate ξ, Eq. (14) yields an implicit solution to Eq. (10)

$$\begin{aligned} Q_k &= Q_I[t - \alpha\beta(Q_k - Q_L x)^{\beta-1}x] + Q_L x \\ &= Q_I[t - F(Q_k - Q_L x)x] + Q_L x \end{aligned} \tag{15}$$

To approximate an explicit solution to Eq. (15), the concept of double decomposition is used to expand $Q_k = \sum_{l=0}^{\infty} Q_{kl}$, and the initial term $Q_{k0} = \sum_{m=0}^{\infty} Q_{k0m}$ in the right side of Eq. (15) (Serrano 2006; Adomian 1994). Thus, the first term in Eq. (15) becomes

$$Q_{k0} = Q_I\left[t - F\left(\sum_{m=0}^{\infty} Q_{k0m} - Q_L x\right)x\right] + Q_L x \tag{16}$$

Now expand $F = \sum_{j=0}^{\infty} F_j$, where F_j is calculated using one of the many algorithms for the Adomian polynomials (Duan and Rach 2011; Rach 2008; Wazwaz 2000). Using the traditional Adomian polynomials about an initial term $f_0 = Q_{k0} - Q_L x = Q_I(t) - Q_L x$ (Adomian 1994), the first few terms are

$$\begin{aligned} F_0(f_0) &= F(f_0) \\ F_1(f_0) &= F_0(f_0)\frac{dF(f_0)}{df_0} \\ F_2(f_0) &= F_1(f_0)\frac{dF(f_0)}{df_0} + \frac{F_0(f_0)^2}{2!}\frac{d^2F(f_0)}{df_0^2} \\ F_3(f_0) &= F_2(f_0)\frac{dF(f_0)}{df_0} + F_1(f_0)F_2(f_0)\frac{d^2F(f_0)}{df_0^2} \\ &\quad + \frac{F_1(f_0)^3}{3!}\frac{d^3F(f_0)}{df_0^3} \qquad \vdots \end{aligned} \tag{17}$$

Combining Eqs. (16) and (17), successively approximate Q_{k0}

$$\begin{aligned} Q_{k00} &= Q_I[t - xF_0(f_0)] + Q_L x, \qquad f_0 = Q_I(t) - Q_L x \\ Q_{k01} &= Q_I\{t - x[F_0(f_0) + F_1(f_0)]\} + Q_L x, f_0 \\ &= Q_{k00}(x,t) - Q_L x \\ Q_{k02} &= Q_I\{t - x[F_0(f_0) + F_1(f_0) + F_2(f_0)]\} + Q_L x, f_0 \\ &= Q_{k01}(x,t) - Q_L x \end{aligned} \tag{18}$$

Note that each term, Q_{k0m}, is evaluated at the previous one, $Q_{k0m-1} - Q_L x$. The convergence of decomposition series has been rigorously established in the mathematical community (Gabet 1992, 1993, 1994; Abbaoui and Cherruault 1994; Cherruault 1989; Cherruault et al. 1992). A convergent decomposition series made of the first few terms usually provides an effective model in practical applications. In most applications of the ADM, the convergence rate is so high that only a few terms are needed to assure an accurate solution. Thus, if, for instance, Q_{k02} is a reasonable approximation to Q_{k0}, then

$$\begin{aligned} Q_k &= Q_{k0} = Q_I\{t - x[F_0(f_0) + F_1(f_0) + F_2(f_0)]\} + Q_L x, \\ f_0 &= Q_{k02}(x,t) - Q_L x \end{aligned} \tag{19}$$

Eq. (19) is the first approximation to the dynamic wave Eqs. (2) and (8). It also constitutes an approximate analytical solution to the nonlinear kinematic wave Eq. (10). Higher-order terms in Eq. (8) are given by

$$Q_i = L_x^{-1}G_j + H_j + K_j + L_x^{-1}J_j L_t Q_{i-1} \tag{20}$$

Similar to Eq. (17), the Adomian polynomials for the nonlinear functions G, H, K, and J in Eqs. (7), (8), and (20) are sequentially generated about an initial term. The first term is given by

$$G_0 = G(Q_I) \qquad H_0 = H(Q_k) \qquad K_0 = K(Q_k) \qquad J_0 = J(Q_I) \tag{21}$$

From Eqs. (20) and (21), derive the first term of the solution

$$Q_0 = Q_k + L_x^{-1}G_0 + H_0 + K_0 + L_x^{-1}J_0 L_t Q_I \tag{22}$$

The second term of the nonlinear functions is given by

$$\begin{aligned} G_1 &= Q_0\frac{dG(g_0)}{dg_0} \\ H_1 &= Q_0\frac{dH(h_0)}{dh_0} \\ K_1 &= Q_0\frac{dK(k_0)}{dk_0} \\ J_1 &= Q_0\frac{dJ(j_0)}{dj_0} \end{aligned} \tag{23}$$

where $g_0 = h_0 = k_0 = j_0 = Q_I$. From Eqs. (20) and (23), derive the second term of the solution

$$Q_1 = L_x^{-1}G_1 + H_1 + K_1 + L_x^{-1}J_1 L_t Q_I \tag{24}$$

The third term of the nonlinear functions is given by

$$\begin{aligned} G_2 &= Q_1\frac{dG(g_0)}{dg_0} + \frac{Q_0^2}{2!}\frac{d^2G(g_0)}{dg_0^2} \\ H_2 &= Q_1\frac{dH(h_0)}{dh_0} + \frac{Q_0^2}{2!}\frac{d^2H(h_0)}{dh_0^2} \\ K_2 &= Q_1\frac{dK(k_0)}{dk_0} + \frac{Q_0^2}{2!}\frac{d^2K(k_0)}{dk_0^2} \\ J_2 &= Q_1\frac{dJ(j_0)}{dj_0} + \frac{Q_0^2}{2!}\frac{d^2J(j_0)}{dj_0^2} \end{aligned} \tag{25}$$

From Eqs. (20) and (24), derive the third term of the solution

$$Q_2 = L_x^{-1}G_2 + H_2 + K_2 + L_x^{-1}J_2 L_t Q_I \tag{26}$$

The fourth term of the nonlinear functions is given by

$$G_3 = Q_2 \frac{dG(g_0)}{dg_0} + Q_1 Q_2 \frac{d^2 G(g_0)}{dg_0^2} + \frac{Q_1^3}{3!} \frac{d^3 G(g_0)}{dg_0^3}$$

$$H_3 = Q_2 \frac{dH(h_0)}{dh_0} + Q_1 Q_2 \frac{d^2 H(h_0)}{dh_0^2} + \frac{Q_1^3}{3!} \frac{d^3 H(h_0)}{dh_0^3}$$

$$K_3 = Q_2 \frac{dK(k_0)}{dk_0} + Q_1 Q_2 \frac{d^2 K(k_0)}{dk_0^2} + \frac{Q_1^3}{3!} \frac{d^3 K(k_0)}{dk_0^3}$$

$$J_3 = Q_2 \frac{dJ(j_0)}{dj_0} + Q_1 Q_2 \frac{d^2 J(j_0)}{dj_0^2} + \frac{Q_1^3}{3!} \frac{d^3 J(j_0)}{dj_0^3} \tag{27}$$

From Eqs. (20) and (24), derive the fourth term of the solution

$$Q_3 = L_x^{-1} G_3 + H_3 + K_3 + L_x^{-1} J_3 L_t Q_I \tag{28}$$

If the magnitude of Q_3 is smaller than a desired resolution, then $Q \approx \sum_{i=0}^{3} Q_i$. Otherwise the calculation may be continued in as described above.

Verification with Independent Numerical Solutions

Exact analytical solutions of the nonlinear kinematic wave and the nonlinear dynamic wave equations are rare. The ADM approximate analytical solutions derived above are verified with the controlled numerical experiments conducted by Szymkiewicz (2010). Assuming $\alpha = 5/3$, $\beta = 3/5$, $Q_L = 0$, $n = 0.03$, $B = 25$ m, $S_0 = 0.0005$, and an inflow hydrograph given by

$$Q_I(t) = q_0 + (q_{\max} - q_0)\left(\frac{t}{t_{\max}}\right) e^{[1-(t/t_{\max})]} \tag{29}$$

where $q_0 = 5$ m^3/s, $q_{\max} = 100$ m^3/s, and $t_{\max} = 4$ h. Fig. 1 shows a comparison between a three-term analytical nonlinear kinematic wave, Eqs. (17)–(19), at $\boldsymbol{x} = 75$ km and the numerical hydrograph calculated by the modified finite-element method according to Szymkiewicz (2010). The time to peak calculated by the two methods is in excellent agreement. The analytical solution seems to better preserve the peak magnitude, in agreement with kinematic wave theory. There appears to be some minor differences in the recession limb possibly because of numerical dissipation. However, the calculation of the analytical hydrograph is much simpler and faster than the numerical one; it requires only a few lines in any standard mathematics software, such as Maple. It is interesting to note that the front of the propagating nonlinear kinematic wave becomes steeper. This occurs because the advection velocity in Eq. (10), $\alpha\beta Q^{\beta-1}$, increases with the flow rate, Q, so that the wave peak moves faster than the lower portions. At some point, the propagating wave may breakdown. For this particular problem, the ADM kinematic wave solution shows signs of instability at prolonged distances of observation(e.g., greater than 100 km), and no smooth profiles of a breaking wave were produced. This is an interesting topic for future research.

Fig. 2 shows a comparison between a four-term analytical nonlinear dynamic wave, Eqs. (20)–(28), at $\boldsymbol{x} = 75$ km and the numerical diffusive hydrograph calculated by the modified finite-element method according to Szymkiewicz (2010). The numerical hydrograph does not include all the terms of the momentum Eq. (2). Nevertheless, it is interesting to note that the peak flow rate and the peak time are very similar in both hydrographs. Including the momentum equation in the analysis causes a decrease in the magnitude of the flow rate at all times. Except for the flood peak, the nonlinear analytical solution exhibits lower flow rates than the numerical solution. The numerical solution also shows higher dispersion. In general, the ADM nonlinear kinematic and nonlinear dynamic wave solutions exemplify the usual features of nonlinear waves, namely its asymmetry with respect to its center of mass, with a sharp rising limb and a flatter recession limb. Linear approximations usually miss these important features. It is also interesting to observe that both the numerical and the analytical hydrographs exhibit errors in the balance of the transported quantity, a fact that

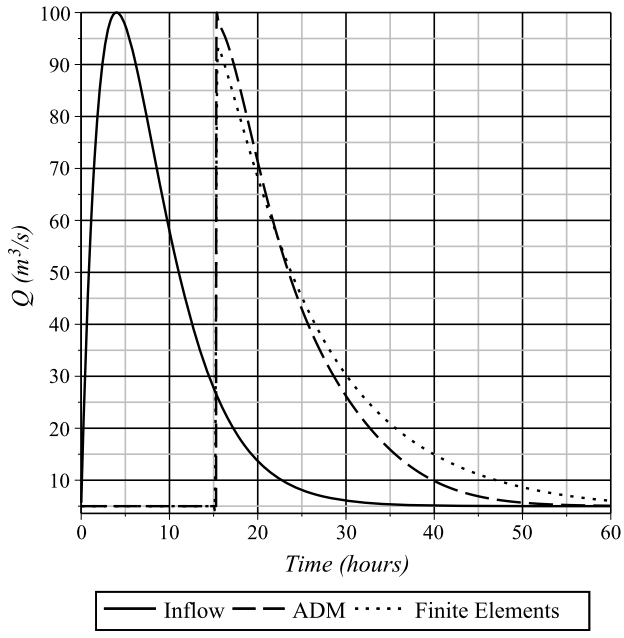

Fig. 1. Analytical versus numerical nonlinear kinematic wave hydrograph at $x = 75$ km (data from Szymkiewicz 2010)

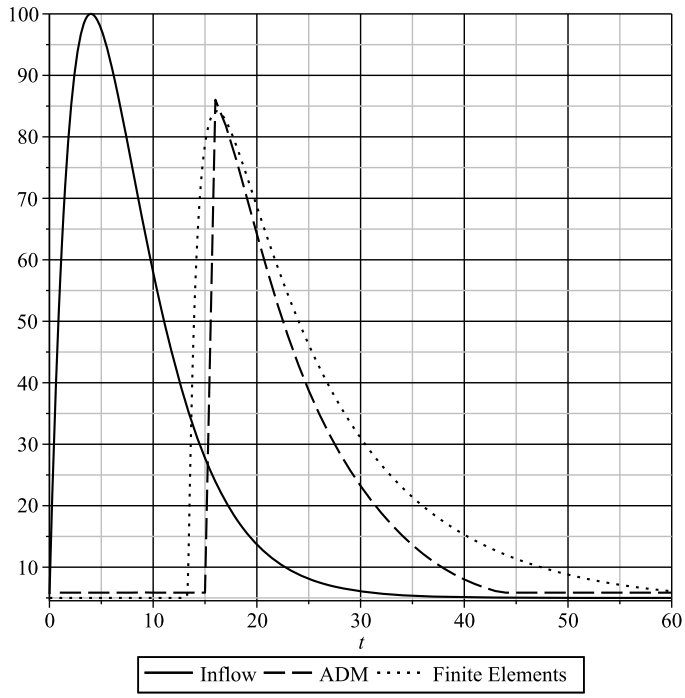

Fig. 2. Analytical nonlinear dynamic wave versus numerical nonlinear diffusive wave hydrograph at $x = 75$ km (data from Szymkiewicz 2010)

has been known for a long time. In other words, the total volume of water leaving the river reach differs from that entering the channel, by about 6% for nonlinear kinematic wave models, 8% for nonlinear diffusion wave models, and perhaps greater for nonlinear dynamic wave models (Szymkiewicz 2010). This is a limitation of the nonlinear models, independent of the method of solution used here. For more detailed analysis of mass and momentum conservation errors in simplified nonlinear models, see Szymkiewicz (2010).

Field Verification in the Schuylkill River in Southeast Pennsylvania

The new approximate analytical solutions to the nonlinear kinematic wave and the nonlinear dynamic wave equations were tested using data from the Schuylkill River in Southeast Pennsylvania. Major towns in the watershed include Pottsville, Reading, Pottstown, Norristown, Conshohocken, and Philadelphia. The river travels approximately 210 km from its headwaters at Tuscarora Springs in Schuylkill County to its mouth at the Delaware River in Philadelphia. The Schuylkill River is the largest tributary of the Delaware River and is a major contributor to the Delaware Estuary. Major tributaries of the Schuylkill, in downstream order, are Mill Creek, the West Creek, Perkiomen Creek, Wissahikon Creek, French Creek, and Tulpehocken Creek. The watershed encompasses an area of approximately 5,200 km^2. The Schuylkill River has been an important source of drinking water in the region for over two centuries. Approximately 1.5 million people receive their drinking water from the Schuylkill River and its tributaries. For the purpose of this application, flow between the station at Norristown, with a watershed drainage area of 4,558 km^2, and the station at Philadelphia, located 21 km downstream and a drainage area of 4,903 km^2 used. In this section, the river flows through a predominantly urban environment that includes residential, industrial, and commercial development. Discharge rate data at these stations are provided online by the U.S. Geological Survey, as described in the bibliography (USGS 2005). The same source provided individual discharge versus cross-sectional area data for the above stations. Using the information at these stations, the following average parameters are adopted: $B = 150$; $n = 0.014$; $S_0 = 0.0006569$; a rating-curve relationship of the form $A = \propto Q^{\beta}$, where A is the channel wetted area (m^2), was fitted with average parameter values $\propto = 4.6$ m$^{2-3\beta}$s$^{\beta}$, and $\beta = 0.594$. The period of analysis included an unusually wet hydrologic year, beginning July 1, 2004.

To account for variable lateral flow, while maintaining a simple, yet nonlinear, model, the lateral flow representation could be modified so as to account for the time variability of effective precipitation during high-intensity storms. For small sub-watersheds, the lateral inflow may be given as

$$Q_L(L,t) = q_0 + \frac{cA_sP_e(t)}{L} \tag{30}$$

where $q_0 = 0.0001$ m^2/s is the constant lateral flow contribution from the groundwater flow estimated from the difference between average baseflow values at the downstream and the upstream stations, respectively; $A_s = 3.45 \times 10^8$ m^2 is the watershed area between the monitoring stations; $L = 21$ km is the distance along the stream between the upstream and downstream stations; $c = 0.2778 \times 10^{-6}$ m $\cdot$ mm^{-1}h $\cdot$ s^{-1} is a units conversion factor; and $P_e(t)$ is the spatially averaged effective precipitation rate in the sub-watershed obtained from daily rainfall rate estimates after the infiltration rate has been subtracted (mm/h). Daily precipitation from rainfall was obtained online from the National Oceanic and Atmospheric Administration's (NOAA) National Climatic Data Center (NOAA 2005). A constant loss rate of 75 mm/day was subtracted from the total daily rainfall values. In Eq. (30), consideration was not given to overland flow storage or surface routing effects.

Since the simulations used daily discharges reported at Norristown (inflow hydrograph, Q_I), a simplified version of the nonlinear kinematic and nonlinear dynamic wave equations was used. In other words, discharges at Philadelphia were approximated with a one-term decomposition term from Eqs. (18) and (22)

$$Q \approx Q_{k0} + L_x^{-1}G_0 + H_0 + K_0 + L_x^{-1}J_0L_tQ_I$$
$$Q_{k0} = Q_I[t - xF_0(f_0)] + Q_Lx, \qquad f_0 = Q_I(t) - Q_Lx \tag{31}$$

where the initial nonlinear functions F_0, G_0, H_0, K_0, and J_0, are given by Eqs. (7), (17) and (21). Fig. 3 displays a comparison between observed and predicted daily flow rates for variable lateral inflow, according to the nonlinear kinematic wave [Eq. (19)], using a one-term decomposition term in Eq. (18). Fig. 4 displays a comparison between observed and predicted daily flow rates for variable lateral inflow, according to the nonlinear dynamic wave [Eq. (31)]. In general, agreement between the observed and predicted flow rates is reasonable. The inclusion of estimates of effective precipitation significantly improved the accuracy of the model with respect to observed flow rates, especially during peak times. The standard deviation of the absolute error between observed and predicted discharge is 24.295 m^3/s for this hydrologic year. It is interesting to know that the greatest portion of the magnitude of discharge is given by the initial nonlinear kinematic wave component, Q_{k0}, which implies that in the lower Schuylkill River the translational components dominated the propagation of flood waves, in agreement with previous research. To better see this, a magnified detail of Figs. 3 and 4 is depicted in Fig. 5 illustrating both the nonlinear kinematic wave and the nonlinear dynamic wave. In general, the nonlinear dynamic wave better predicts the flow rate, during peak times and especially during recession and low-flow periods. Thus, while both models are based on simple approximate analytical solutions and their implementation is easy, the nonlinear kinematic wave equation model requires less data and could be useful in preliminary analyses with scarce data.

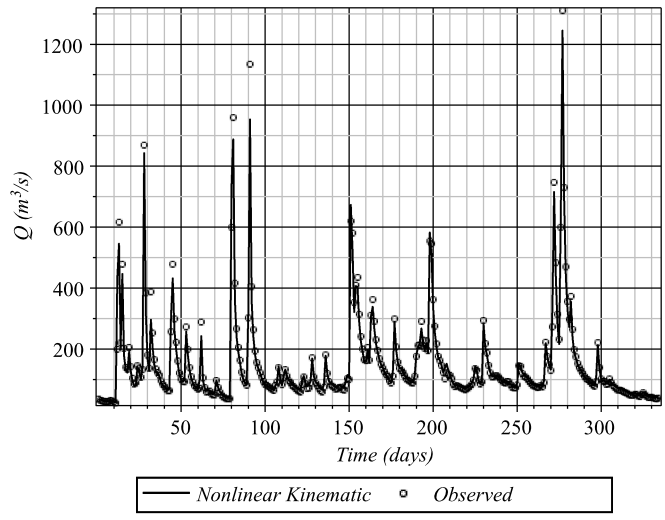

Fig. 3. Predicted discharge at Philadelphia according to analytical nonlinear kinematic wave during one hydrologic year beginning July 2004

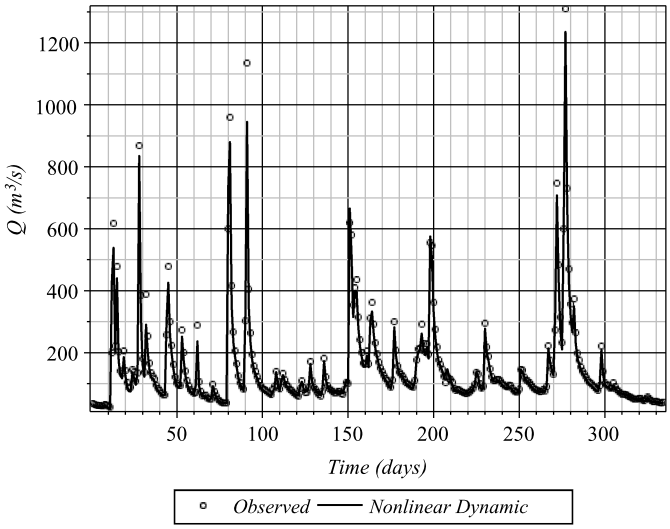

Fig. 4. Predicted discharge at Philadelphia according to analytical nonlinear dynamic wave during one hydrologic year beginning July 2004

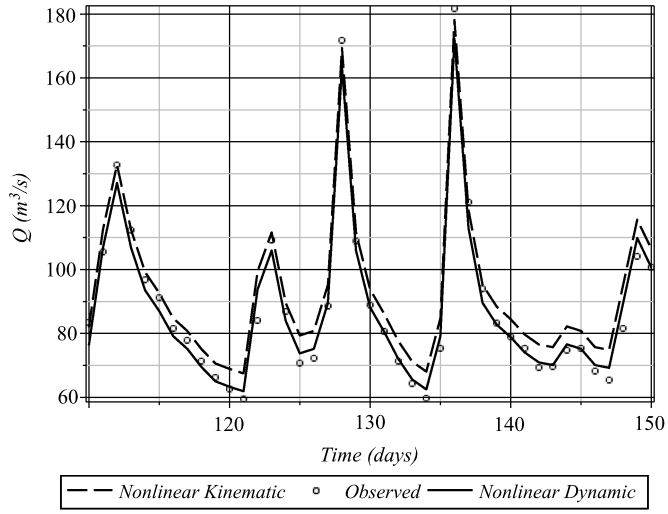

Fig. 5. Detail of Figs. 3 and 4 illustrating the nonlinear kinematic wave and the nonlinear dynamic wave

Summary and Conclusions

New approximate analytical solutions of the nonlinear kinematic wave and the nonlinear dynamic wave equations in rivers were introduced. The solutions were derived by combining ADM, the method of characteristics, the concept of double decomposition, and successive approximation. The new solutions compared favorably with independent simulations using the modified finite-element method, and field data at the Schuylkill River near Philadelphia. The new solutions are easy to apply and permit the efficient forecast of nonlinear kinematic and nonlinear dynamic flood waves. Advantages include a simple approach for preliminary hydrologic forecast under scarce data; an analytic description of flow rates and gradients; a description of state variables continuously over the spatial and temporal domain; minimal complications from stability and numerical roundoff; no need of a numerical grid or the handling of large sparse matrices; no need of specialized software, since all calculations may be done with standard mathematics or spreadsheet programs. The new solutions may also serve as a potential source of reference data for testing new numerical methods and algorithms proposed for the open channel flow equations. In general, the ADM nonlinear kinematic and nonlinear dynamic wave solutions exhibit the usual features of nonlinear waves, namely its asymmetry with respect to its center of mass, with sharp rising limbs and flatter recession limbs. Linear approximations of the governing equations usually miss these important features of nonlinear waves. The greatest portion of the magnitude of discharge is given by the initial nonlinear kinematic wave component, Q_{k0}, which implies that in the lower Schuylkill River the translational components dominate the propagation of flood waves, in agreement with previous research. The nonlinear dynamic wave better predicts the flow rate, during peak times and especially during recession and low-flow periods. Thus, while both the nonlinear kinematic and the nonlinear dynamic wave models are based on simple approximate analytical solutions and their implementation is easy, the nonlinear kinematic wave equation model requires less data and less computational effort.

Acknowledgments

Numerical data for the comparison of the ADM models in Figs. 1 and 2 was kindly provided via personal communication by Professor Romuald Szymkiewicz from the Gdańsk University of Technology, Poland. Streamflow data for the present study was provided online by the U.S. Geological Survey. Rainfall information for the present study was provided online by the U.S. National Oceanic and Atmospheric Administration (NOAA).

References

Abbaoui, K., and Cherruault, Y. (1994). "Convergence of Adomian's method applied to differential equations." *Comput. Math. Appl.*, 28(5), 103–109.

Adomian, G. (1983). *Stochastic systems*, Academic Press, New York.

Adomian, G. (1986). *Non-linear stochastic operator equations*, Academic Press, New York.

Adomian, G. (1991). "A review of the decomposition method and some recent results for nonlinear equations." *Comput. Math. Appl.*, 21(5), 101–127.

Adomian, G. (1994). *Solving frontier problems in physics-the decomposition method*, Kluwer Academic, Boston.

Adomian, G. (1995). "Analytical solution of Navier-Stokes flow of a viscous compressible fluid." *Found. Phys. Lett.*, 8(4), 389–400.

Aronica, G., Tucciarelli, T., and Nasello, C. (1998). "2D multilevel model for flood wave propagation in flood-affected areas." *J. Water Resour. Plann. Manage.*, 10.1061/(ASCE)0733-9496(1998)124:4(210), 210–217.

Bates, P. D., Horritt, M. S., and Fewtrell, T. J. (2010). "A simple inertial formulation of the shallow water equations for efficient two-dimensional flood inundation modelling." *J. Hydrol.*, 387(1–2), 33–45.

Cappelaere, B. (1997). "Accurate diffusive wave routing." *J. Hydraul. Eng.*, 10.1061/(ASCE)0733-9429(1997)123:3(174), 174–181.

Cherruault, Y. (1989). "Convergence of Adomian's method." *Kybernetes*, 18(2), 31–38.

Cherruault, Y., Saccomardi, G., and Some, B. (1992). "New results for convergence of Adomian's method applied to integral equations." *Math. Comput. Modell.*, 16(2), 85–93.

Chow, V. T. (1959). *Open channel hydraulics*, McGraw-Hill, Tokyo.

Chow, V. T., Maidment, D. R., and Mays, L. W. (1988). *Applied hydrology*, McGraw-Hill, New York.

de Almeida, G. A. M., and Bates, P. (2013). "Applicability of the local inertial approximation of the shallow water equations to flood modeling." *Water Resour. Res.*, 49(8), 4833–4844.

de Almeida, G. A. M., Bates, P. D., Freer, J., and Souvignet, M. (2012). "Improving the stability of a simple formulation of the shallow water equations for 2D flood modelling." *Water Resour. Res.*, 48(5), in press.
Di Silvio, G. (1969). "Flood wave modification along prismatic channels." *J. Hydraul. Div.*, 95, 1589–1614.
Dooge, J. C. I., and Napiorkowski, J. J. (1987). "Applicability of diffusion analogy in flood routing." *Acta Geophys. Pol.*, 35(1), 65–75.
Duan, J.-S., and Rach, R. (2011). "A new modification of the Adomian decomposition method for solving boundary value problems for higher-order nonlinear differential equations." *Appl. Math. Comput.*, 218(8), 4090–4118.
Ferrick, M. G. (1985). "Analysis of river wave types." *Water Resour. Res.*, 21(2), 209–220.
Ferrick, M. G., Bilmes, J., and Long, S. E. (1984). "Modeling rapidly varied flow in tailwaters." *Water Resour. Res.*, 20(2), 271–289.
Gabet, L. (1992). "Equisse d'une théorie décompositionnelle et application aux equations aux dérivées partialles." Ph.D. dissertation, École Centrale Paris, Paris, France (in French).
Gabet, L. (1993). "The decomposition method and linear partial differential equations." *Math. Comput. Modell.*, 17(6), 11–22.
Gabet, L. (1994). "The decomposition method and distributions." *Comput. Math. Appl.*, 27(3), 41–49.
Hromadka, T. V., and Yen, C. C. (1986). "A diffusion hydrodynamic model (DHM)." *Adv. Water Resour.*, 9(3), 118–170.
Jeffrey, A. (2003). *Applied partial differential equations*, Academic Press, New York.
Jin, M., and Fread, D. (1997). "Dynamic flood routing with explicit and implicit numerical solution schemes." *J. Hydraul. Eng.*, 10.1061/(ASCE)0733-9429(1997)123:3(166), 166–173.
Kazezyilmaz-Alhan, C., and Medina, M., Jr. (2007). "Kinematic and diffusion waves: Analytical and numerical solutions to overland and channel flow." *J. Hydraul. Eng.*, 10.1061/(ASCE)0733-9429(2007)133:2(217), 217–228.
Lamberti, P., and Pilati, S. (1996). "Flood propagation models for real-time forecasting." *J. Hydrol.*, 175(1–4), 239–265.
Lighthill, M. J., and Whitham, G. B. (1955). "On kinematic waves. I: Flood movement in long rivers." *Proc. R. Soc. London, Ser. A*, 229(1178), 281–316.
Martin, J. L., and McCutcheon, S. C. (1999). *Hydrodynamics and transport for water quality modeling*, Lewis, Boca Raton, FL.
Moramarco, T., Pandolfo, C., and Singh, V. P. (2008). "Accuracy of kinematic wave and diffusion wave approximations for flood routing. I: Steady analysis." *J. Hydrol. Eng.*, 10.1061/(ASCE)1084-0699(2008)13:11(1089), 1089–1096.
Moris, E. M., and Woollhiser, D. A. (1980). "Unsteady one-dimensional flow over a plane: Partial equilibrium and recession hydrographs." *Water Resour. Res.*, 16(2), 355–360.
NOAA (National Oceanic and Atmospheric Administration). (2005). "NOAA National Climatic Data Center." ⟨http://www.ncdc.noaa.gov⟩ (Jun. 2005).
Philipp, A., Liedl, R., and Wöhling, T. (2012). "Analytical model of surface flow on hillslopes based on the zero inertia equations." *J. Hydraul. Eng.*, 10.1061/(ASCE)HY.1943-7900.0000519, 391–399.
Ponce, V. M. (1986). "Diffusion wave modelling of catchment dynamics." *J. Hydraul. Eng.*, 10.1061/(ASCE)0733-9429(1986)112:8(716), 716–727.
Ponce, V. M., Li, R.-M., and Simons, D. B. (1978). "Applicability of kinematic and diffusion models." *J. Hydraul. Div.*, 104(HY3), 353–360.
Ponce, V. M., and Simons, D. B. (1977). "Shallow wave propagation in open channel flow." *J. Hydraul. Div.*, 103(HY12), 1461–1476.
Rach, R. (2008). "A new definition of the Adomian polynomials." *Kybernetes*, 37(7), 910–955.
Rach, R. (2012). "A bibliography of the theory and applications of the Adomian decomposition method, 1961–2011." *Kybernets*, 41(7/8), 1087–1148.
Rach, R., Wazwaz, A.-M., and Duan, J.-S. (2013). "A reliable modification of the Adomian decomposition method for higher-order nonlinear differential equations." *Kybernetes*, 42(2), 282–308.
Serrano, S. E. (2006). "Development and verification of an analytical solution for forecasting nonlinear kinematic flood waves." *J. Hydrol. Eng.*, 10.1061/(ASCE)1084-0699(2006)11:4(347), 347–353.
Serrano, S. E. (2010). "Hydrology for engineers, geologists, and environmental professionals." *An integrated treatment of surface, subsurface, and contaminant hydrology*, HydroScience, Ambler, PA.
Serrano, S. E. (2011). "Engineering uncertainty and risk analysis." *A balanced approach to probability, statistics, stochastic models, and stochastic differential equations*, HydroScience, Ambler, PA.
Singh, V. P. (1996). *Kinematic wave modeling in water resources: Surface water hydrology*, Wiley, New York.
Singh, V. P., and Aravamuthan, V. (1996). "Errors of kinematic-wave and diffusion-wave approximations for steady-state overland flows." *Catena*, 27(3–4), 209–227.
Szymkiewicz, R. (2010). "Numerical modeling in open channel hydraulics." *Water science and technology library*, Springer, New York.
Tsai, C. W. (2003). "Applicability of kinematic, noninertia, and quasi-steady dynamic wave models to unsteady flow routing." *J. Hydraul. Eng.*, 10.1061/(ASCE)0733-9429(2003)129:8(613), 613–627.
Tsai, C. W., and Yen, B. C. (2004). "Shallow water propagation in convectively accelerating open-channel flow induced by tailwater effect." *J. Eng. Mech.*, 10.1061/(ASCE)0733-9399(2004)130:3(320), 320–336.
USGS. (2005). "USGS water data for the nation." National Water Information System (NWIS), ⟨http://waterdata.usgs.gov/nwis⟩ (Jun. 2005).
Vieira, J. H. D. (1983). "Conditions governing the use of approximations for the Saint-Venant equations for shallow surface water flow." *J. Hydrol.*, 60(1–4), 43–58.
Wazwaz, A.-M. (2000). "A new algorithm for calculating Adomian polynomials for nonlinear operators." *Appl. Math. Comput.*, 111(1), 33–51.
Woolhiser, D. A., and Liggett, J. A. (1967). "Unsteady, one-dimensional flow over a plane—The rising hydrograph." *Water Resour. Res.*, 3(3), 753–771.
Xia, R. (1995). "Impact of coefficients in momentum equation on selection of inertial models." *J. Hydraul. Res.*, 32(4), 615–621.